Ensemble forecast spread induced by soil moisture changes over mid-south and neighbouring mid-western region of the USA

By ARTURO I. QUINTANAR[1]* and REZAUL MAHMOOD[2,3,4], [1]*Centro de Ciencias de la Atmosfera, Universidad Nacional Autónoma de México, Circuito Exterior, Ciudad Universitaria, México D.F. 04510, México*; [2]*Meteorology Program, Western Kentucky University, 1906 College Heights Blvd., Bowling Green KY 42101-1066, USA*; [3]*Department of Geography and Geology, Western Kentucky University, 1906 College Heights Blvd., Bowling Green KY 42101-1066, USA*; [4]*Kentucky Climate Center, Western Kentucky University, 1906 College Heights Blvd., Bowling Green KY 42101-1066, USA*

ABSTRACT

This study investigated the potential impact of soil moisture perturbations on the statistical spread of an ensemble forecast for three different synoptic events during the summer of 2006. Soil moisture was perturbed from a control simulation to generate a 12 member ensemble with six drier and six moister soils. The impacts on the near-surface atmospheric conditions and on precipitation were analysed. It was found, as previous studies have confirmed, that soil moisture can change the spatial and temporal distribution of precipitation and of the overlying circulation. It was found that regardless of the conditions in synoptic forcing, temperature, relative humidity and horizontal wind field exhibited a spatial correlation coefficient (R) close to one with respect to the control simulation. Vertical velocity, however, showed a marked decrease in R down to 0.4 as the precipitation activity increased. For vertical velocity, however, this quantity grew to near 1.0 consistent with R near zero and standard deviations very close to that of the control. These results suggested a more complex picture in which soil moisture perturbations played a major role in modifying precipitation and the near-surface circulation but did not broaden the statistical spread of trajectories in phase space of all variables.

Keywords: soil moisture, ensemble forecast, atmosphere-soil interactions, spatial correlation, pattern correlation

1. Introduction

The coupling between the atmosphere and land processes can impact atmospheric forecasts on almost every temporal and spatial scales of concern to society. At the root of this interaction lies evaporation and transpiration from bare soil and vegetation and the manner in which soil moisture exerts control over it (Pielke, 2001). While there may be other factors that control evaporation and transpiration (e.g. atmospheric conditions, plant physiology and soil characteristics), to a first order, soil moisture seems to largely dominate evaporation in transitional wet–dry soil regimes in middle latitudes (Koster et al., 2004; Senevirante et al., 2006; Teuling et al., 2006).

It is well-known that soil moisture can affect atmospheric conditions that lead to convection and rainfall (Chang et al., 2009; Chen and Avissar, 1994; Crook, 1996; Diak et al., 1986; Dong et al., 2007; Fast and McCorcle, 1991; Taylor et al., 1997). However, numerous potential paths or links that connect soil moisture and precipitation are still largely unknown as the processes and feedbacks involved are non-linear and difficult to identify in an observational and modelling set up (Santanello et al., 2009). There is evidence that weather variability on several time scales over continental land masses is linked or partially controlled by the local land–atmosphere interactions and the feedbacks that ensue (Betts et al., 1996; Ek and Mahrt, 1994; Findell and Eltahir, 2003; Koster et al., 2004; Yang et al., 2004). In addition, the sign and nature of soil moisture-precipitation feedbacks can change according to the region and to the time scales of interest with effects observable even at diurnal time scales (Findell and Eltahir, 2003; Schär et al., 1999; Taylor

*Corresponding author.
email: arturo.quintanar@atmosfera.unam.mx

1

et al., 1997). Investigations, at local and regional scales, on the strength and nature of processes linking soil moisture dynamics, boundary layer processes and ultimately precipitation are required to be included in the current modelling efforts (Legates et al., 2011; Santanello et al., 2011).

Observational evidence of positive soil moisture-precipitation feedback in semi-arid regions can be found in research conducted in the African Sahel which suggests large precipitation gradients are the result of convective-scale systems exposed to soil moisture anomalies (Taylor et al., 1997, 2003). Negative feedback is also observed in this region over wet soils from antecedent precipitation, where afternoon convective storms are suppressed by increased subsidence from localised mesoscale circulations induced by soil moisture gradients (Ookouchi et al., 1984; Taylor and Ellis, 2006; Taylor et al., 2007). Another aspect of the observational problems found with soil moisture is that despite recent progress with retrieval methods using satellite data to obtain soil moisture, paucity in observed soil moisture and soil temperature data over the continents has impeded the production of reliable assimilated soil moisture products, particularly at deeper levels (Balsamo et al., 2007; Capprini and Castelli, 2004; Mahmood and Hubbard, 2004). Hence, there is an inherent uncertainty in the knowledge of actual soil moisture content globally and also at continental scales over the United States.

Given the potential for soil moisture to change the energy partition at the surface and penetrative convection, it is conceivable that deterministic forecasts can be sensitive to perturbations in initial conditions that include soil moisture uncertainty. Operational ensemble prediction systems may benefit from inclusion of this uncertainty to produce a more appropriate spread.

Ensemble forecasts are, generally, the result of perturbed atmospheric initial conditions using one or several atmospheric models that differ in their dynamical core design, spatial resolution or the implementation of model physics, particularly in the parameterisation of convective processes and the interactions with the boundary layer (Hamill and Colucci, 1997; Palmer et al., 2004; Pielke, 2001; Sasamori, 1970; Stensrud et al., 2000; Toth et al., 1997; Tracton and Kalnay, 1993). The objective of ensemble forecasting is to broaden the statistical spread of atmospheric states such that the true atmospheric state can be drawn from that population with equal probability. In other words, if the spread were too small then the true atmospheric state would become an outlier rendering the ensemble average useless for operational forecasts (Kalnay, 2003). Recently, with regard to regional atmospheric models and short-range weather forecasting, it has been pointed out that surface processes over land can also have an important contribution to the ensemble spread (Aligo et al., 2007; Sutton et al., 2006).

Sutton et al. (2006) used two soil moisture analyses originating from two different land surface models (LSM) including the stand-alone Noah LSM (Chen and Dudhia, 2001) and the stand-alone Mosaic LSM (Koster and Suarez, 1996). The LSMs were forced with exactly the same meteorological data but produced different soil moisture distributions due to different design. The authors found that the Mosaic LSM produced drier soil moisture analyses. Sutton et al. (2006) used these two soil moisture sets to force the Weather Research and Forecasting Model (WRF) with the Advanced Research WRF (ARW) dynamical core to produce 24-h ensemble forecasts at 5 km resolution for six different synoptic conditions. All of them were characterised by a weak synoptic forcing during summer over the Central and South Eastern United States. The results showed significant differences in near-surface temperature and precipitation and suggested that the variability induced by soil moisture differences can, in fact, add to the spread of ensemble members and improve on the short-range weather forecasting which usually suffers from excessive similarity among significant number of ensemble members.

Aligo et al. (2007) took a closer look at the problem adding more cases of weakly and strongly forced summer synoptic events to force the WRF/ARW model for a 24-h integration at 4 km resolution. To evaluate the spread of the ensemble, they used relative operating characteristic curves (ROC) and a rank histogram to test the ensemble forecast system. Their results showed that while the forecast skill of the ensemble improved, the spread for weakly forced conditions was only marginally better. Their study suggested that a better ensemble set can be constructed from perturbing other aspects such as atmospheric initial conditions. Perturbations applied only to soil moisture might not be enough to produce sufficient variability to the precipitation forecast. We note that both Sutton et al. (2006) and Aligo et al. (2007) constructed their initial soil moisture fields from operational models such as North American Mesoscale Model (NAM) and Rapid Update Cycle (RUC). It was suggested by Aligo et al. (2007) that the sensitivity to soil moisture might be compromised by the way in which soil moisture was initialised and therefore it continues to be a matter of research to establish the correct procedures to initialise soil moisture for ensemble weather forecasting.

Quintanar et al. (2008) used the regional model MM5 coupled to the Noah LSM (Chen and Dudhia, 2001) to study precipitation sensitivity to soil moisture specification during June 2006 in Kentucky. They found that the near-surface wind field and precipitation patterns were significantly sensitive to soil moisture perturbations during three different synoptic events. In agreement with results from Sutton et al. (2006) precipitation values were mostly affected by soil moisture changes when vertical velocity exceeded certain

thresholds. It was plausible that under these conditions soil moisture perturbations could broaden the precipitation variance of ensemble members and of near-surface atmospheric variables used in air quality and transport studies.

The present work is a follow up of and complimentary to the work by Sutton et al. (2006), Aligo et al. (2007) and Quintanar et al. (2008) and hence provided additional insight for soil moisture impacts on ensemble spread. Specifically, this paper assessed the impacts of soil moisture changes on ensemble spread for three precipitation events forced by different synoptic atmospheric conditions on 11, 17 and 22 June 2006 as described in Section 3.

Sutton et al. (2006) and Aligo et al. (2007) have primarily focused on ensemble spread of precipitation and temperature due to changes in soil moisture. In the current research, in addition to precipitation and temperature, we have also evaluated ensemble spread of relative humidity, horizontal and vertical wind. We have included these variables in this study because they are quite useful in explaining precipitation changes due to changes in soil moisture (e.g. Quintanar et al., 2008). Another objective of this study was to diagnose the temporal dispersion of the ensemble member population from a control simulation using a time-dependent measure of spread when soil moisture was subjected to variations.

This representation of spread of members was based on four statistical measures: normalised centred root-mean square difference (RMSD), the normalised standard deviation (σ), the normalised bias (B) and the spatial correlation coefficient (R) (Taylor, 2001). These statistics have been successfully and extensively used to test forecast skill of global and regional atmospheric models (e.g. Duffy et al., 2006; Li et al., 2008; Tjernström et al., 2005) and to evaluate the strengths and weaknesses of reanalysis data (e.g. Bosilovich et al., 2008). It has also been used frequently in research involving coupled hydrodynamic-ecosystem models of increasing complexity (e.g. Jolliff et al., 2009). A succinct way of grasping how the model's ensemble simulations evolve in such a high-dimensional phase space is to look at the pattern statistics involving the above-mentioned quantities. The time behaviour of these measures was used to reveal the evolution of the model-atmosphere and explain under which conditions perturbations in soil moisture alone were expected to create variability in different meteorological fields.

2. Data and methodology

2.1. The MM5 model

In this study, the Penn State University/UCAR regional atmospheric model MM5 version 3.7, coupled to the Noah LSM was used (see Chen and Dudhia, 2001). The Noah LSM uses four soil layers (10, 30, 60 and 100 cm thickness) to predict soil temperature, soil water/ice and snow cover. The total soil depth is 2 m with the root zone in the upper 1 m. The Kain–Fritsch (Kain, 2004) convection parameterisation scheme was used which included a shallow convection scheme for the coarse grid simulations. For higher resolution simulations the convection parameterisation was turned off. Specification of turbulent fluxes was performed using the MRF turbulent scheme (Hong and Pan, 1996).

2.1.1. Domain configuration. Figure 1 shows the outer domain at 12 km grid spacing covering a portion of the South Central United States with approximate dimensions of 1600×1000 km. Also shown is the inner domain at 4 km grid spacing which encompassed the Ohio River valley with Kentucky at its centre with approximate dimensions of 800×500 km. Both domain projections (Lambert conformal) were centred at 37.1°N, 86.7°W. Here, a one-way interaction mode between outer and inner domains was chosen to simulate three periods in June as explained in the next section. In this way, the response of the model to soil moisture changes within the inner domain can be assessed in isolation from the forcing at the lateral walls of the same domain. In the vertical, 31 levels were used for both outer and inner domains with 15 levels below 800 hPa to obtain higher vertical resolution within the boundary layer. In the remaining sections all soil moisture changes and results pertain to the higher resolution inner domain.

2.1.2. MM5 configuration. The MM5 is initialised for three periods in 11, 17 and 22 June 2006. Control and soil anomaly experiments started at 1200 UTC for all three periods with each simulation lasting 24 h. The time periods were chosen so that the most significant precipitation
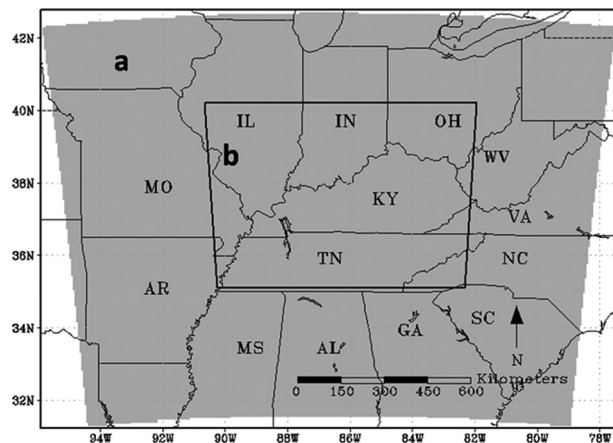

Fig. 1.   One-way nested computational domains centred about Kentucky: (a) outer and (b) inner domain.

events that occurred over the domain were captured (Quintanar et al., 2008). Both, the MM5 and the Noah LSM are initialised with NCEP final reanalysis data (FNL) at $1° \times 1°$ horizontal resolution and updated every 6 h (http://dss.ucar.edu/datasets/ds083.2/). These data sets include soil moisture data at the same four soil levels mentioned previously for the Noah LSM. Additional high resolution (30 s) land use land cover was provided from a 25 category United States Geological Service (USGS) data archive used by the TERRAIN interpolation stage of MM5 to the model's computational grid (http://www.mmm.ucar.edu/mm5/).

In order to generate the soil moisture anomaly from those given in the control run (CTRL), the data in the initialisation files were changed for the four levels of the LSM by the same amount in absolute terms for the entire horizontal computational domain and for the four daily updates available during the 24 h simulations. Thus, for the DRY anomalous experiments, six values of volumetric soil moisture below CTRL values were used: 0.025, 0.05, 0.075, 0.10, 0.125 and 0.15. For WET experiments soil moisture values were increased by the same steps of six increments. The intent of inclusion of extreme soil moisture perturbations ($0.15 \, m^3 \, m^{-3}$) was not to explore impacts of large daily variations (within 24-h simulation period) of soil moisture (SM) on precipitation and planetary boundary layer atmosphere. It was rather to see model and atmospheric responses to extremely high or low soil moisture contents and their impacts on ensemble forecasts. Note, North American Regional Reanalysis (NARR) data suggests that soil moisture for the study periods were relatively high. Drying or wetting of the soil uniformly over the entire domain can still result in inhomogeneous thermal forcing at the surface because the land use and the vegetation cover were not uniform. In addition, changing of soil moisture uniformly can maintain the horizontal gradients approximately the same for all simulations (e.g. Ookouchi et al., 1984). In this study, soil moisture was perturbed only at initial time and allowed to evolve over simulation period. The resulting soil moisture perturbation did not disappear in the area average sense, for the duration of the simulation (not shown). In this study, the soil moisture simulated in the CTRL run was taken as our reference. No attempt was made at this stage to obtain a CTRL simulation close to the reanalysis data.

2.2. Measures of ensemble spread

As stated earlier, the objective in this study was to characterise the evolution of the model ensemble realisations from the control simulation and each perturbation in soil moisture as these traverse different regions of phase space (Kalnay, 2003). One simple way of obtaining this characterisation is to use simple spatial pattern correlations and root mean square differences as measures of the 'distance' in phase space and thus of the ensemble spread. In order to characterise the spread as a function of time between the CTRL simulation and the ensemble members, four statistical measures were used to obtain a spatial distance between ensemble members. They include: the normalised centred or unbiased root-mean square difference RMSD′, the normalised standard deviation (s), the normalised bias (B) and the spatial pattern correlation coefficient (R). RMSD′ is expressed as follows:

$$\text{RMSD}' = \sigma_C^{-1} \left\{ \frac{1}{N} \sum_{n=1}^{N} \left[(C_n - \overline{C}) - (E_n - \overline{E}) \right]^2 \right\}^{1/2}$$

where C and E refers to control and ensemble, the overbar for C and E refers to the spatial area average of a meteorological variable in the control and the ensemble average of a meteorological variable for a soil moisture perturbation experiment, respectively. Correspondingly, C_n and E_n refer to variables evaluated at the nth grid point over a horizontal domain and N refers to the total number of points there. σ_C is the standard deviation of the control run. The RMSD′ is also known as unbiased (Jolliff et al., 2009) since it does not contain any information about the spatial bias between two horizontal fields (Jolliff et al., 2009; Taylor, 2001). The normalised standard deviation can be presented as:

$$\sigma = \frac{\sigma_E}{\sigma_C}$$

where σ_E is the standard deviation of the ensemble mean. The normalised bias defined as the difference of the means of two area averaged fields divided by the standard deviation of the CTRL simulation can be shown as follows:

$$B = \frac{\overline{C} - \overline{E}}{\sigma_C}$$

The spatial correlation coefficient R that measures the degree of phase agreement between two fields is:

$$R = \sigma_C^{-1} \sigma_E^{-1} \frac{1}{N} \sum_{n=1}^{N} (C_n - \overline{C})(E_n - \overline{E})$$

Based on the above statistical measures it possible to obtain additional relationships as suggested by Taylor (2001):

$$\text{RMSD}'^2 = 1 + \sigma^2 - 2\sigma R$$
$$\text{RMSD}^2 = RMSD'^2 + B^2$$

where RMSD is the total root-mean square difference. The RMSD′ is equal to the total RMSD when the mean area average for the CTRL and the ensemble simulations coincide (i.e. $\overline{C} = \overline{E}$). Moreover, when the standard deviation of the CTRL and the ensemble simulations are identical

(i.e. $\sigma = 1$) then RMSD′ and R contain the same amount of information. As shown later, except for vertical velocity, many of the analysed variables reported σ very close to unity. For this reason, instead of using the well-known diagrams proposed by Taylor (2001) as a summary, it was decided to present only RMSD′, σ and B as time series diagrams to render the time evolution of the ensemble clearer.

3. Results and discussion

The synoptic conditions that characterised precipitation events on 11, 17 and 22 June 2006 have been discussed at length in Quintanar et al. (2008). June 11 was a case that involved a stationary front located over Northern Kentucky, West Virginia and North Carolina. This frontal event produced conditions for localised convective activity and precipitation at this time over Central and Eastern Kentucky. On 17 June, a strong low-level jet developed to the west of Kentucky transporting moisture from the Gulf of Mexico. Precipitation in this period was located to the west of Kentucky and over Tennessee. On 22 June, a cold front moved over Kentucky producing precipitation over Central and Western Kentucky. The model captured the 11 June accumulated precipitation and to some extent that of 17 June. However, the 22 June precipitation was not well represented (Quintanar et al., 2008).

In order to obtain an initial idea of the model's response to soil moisture changes, the following sections are devoted to discuss the response in terms of precipitation, wind field and soil moisture. To gain further insight into the model's sensitivity to soil moisture changes, the time evolution of the above-mentioned metrics of selected two-dimensional fields are presented in the following sub-sections.

3.1. 11 June 2006

Figure 2a shows the 24 h accumulated precipitation for the CTRL simulation for this period. Precipitation occurred over most of Kentucky and portions of Southern Indiana and Ohio. Large precipitation amount of up to 50–60 mm were predicted by the model in localised bands oriented in a northwest and southeast direction over eastern and Central Kentucky. Elsewhere, 24-h total precipitation ranged from 10 to 40 mm over most of Kentucky. In addition, Fig. 2a shows 24-h average wind pattern at 960 hPa which was dominated by southwesterly winds over Tennessee and South Central Kentucky and easterly and north easterly winds over Ohio and Indiana, respectively.

Figure 2b shows the sensitivity in terms of precipitation difference between the CTRL simulation and the ensemble average of six dry soil moisture simulations (DRY). The response in precipitation and wind field at 960 hPa was localised over South Central and Western Kentucky. For
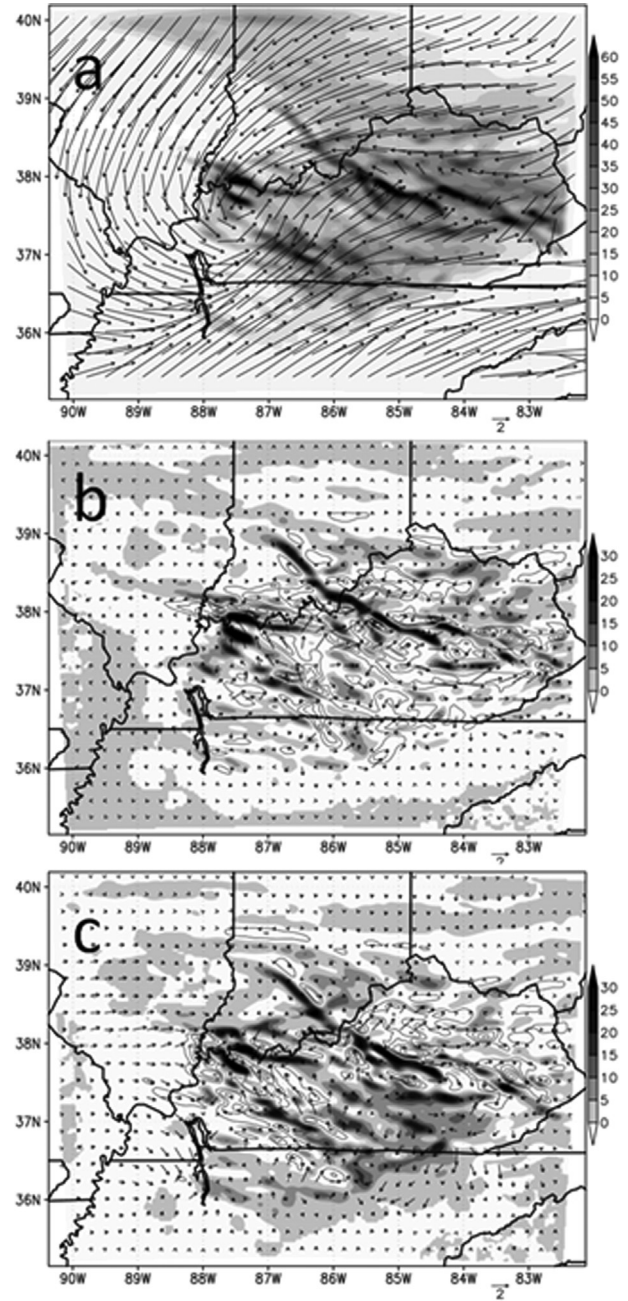

Fig. 2. (a) Twenty-four hour accumulated precipitation (mm) for the CTRL run from 11 June 1200 UTC to 12 June 1200 UTC; (b) CTRL minus the ensemble average of DRY simulations and (c) for the CTRL minus the ensemble average of WET simulations. Shading refers to positive rainfall intensity while white regions and dashed lines denote negative rainfall intensity. Plotted also is the 24 h average of horizontal wind field (vector scale 2 m s^{-1}) at 960 hPa for that period.

CTRL - DRY differences, dark shaded areas in this figure corresponded to regions where precipitation in the CTRL simulation was larger than the DRY ensemble ranging from

2 mm near the domain lateral walls to 25 mm where precipitation was more intense in the CTRL. This was indicative of a positive feedback in these regions. White areas (with contour lines) represented regions where reduction of soil moisture from the CTRL run resulted in an increase in precipitation and thus a negative feedback. In this case, precipitation increased from less than 1 mm in Northern Tennessee, Central Kentucky and Southern Illinois to about 10 mm near the regions of larger precipitation in the CTRL.

Figure 2c shows differences in precipitation between the CTRL simulation and the ensemble average of six wet soil moisture experiments (WET). In this case, for CTRL – WET differences, dark shaded areas in the figure indicate larger precipitation values in the CTRL compared to the WET ensemble. Hence, it also represents a negative feedback effect. Decreases in precipitation ranged from 5 mm in Northern Tennessee, to about 20 mm South Central Kentucky. It was noted, as in the above DRY case, that larger positive precipitation differences were co-located along precipitation bands with values of up to 30 mm in decreased precipitation from the CTRL simulation. Overall, these DRY and WET simulations suggests more complex and non-linear interactions between changes in soil moisture and response of precipitation.

The reasons for the negative soil moisture – precipitation feedback found in our experimental setting are difficult to discern given rather strong frontal influence. Nevertheless, an analysis was conducted using Convectively Available Potential Energy (CAPE), PBL height minus lifting condensation level (LCL) and PBL height minus level of free convection (LFC). CAPE, LCL and LFC are computed for DRY and WET cases using the maximum equivalent potential temperature value below 3000 m. CAPE for the CTRL simulation at three different times for 11 June, including, at 1600 UTC (1100 LST), 2000 UTC (1500 LST) and 0000 UTC (1900 LST) were completed. Results obtained from 11 June apply to 17 and 22 June events as well. We found that CAPE was sensitive to soil moisture changes from morning to afternoon (not shown). As expected, initially, the CTRL – DRY simulation exhibits larger CAPE for the CTRL simulation but regions of negative differences appear to increase particularly in the southern part of the domain in Kentucky, and Tennessee later in the afternoon. This is consistent with the observed negative feedback found in accumulated precipitation patterns. Similarly, the CTRL – WET difference exhibited an opposite pattern with respect to its DRY counterpart but again showing regions where the difference was possitive in agreement with previously found negative feedback.

We further analysed the events in 11 June by looking at the differences between PBL height and LCL and PBL height and LFC (not shown). It has been argued in the literature (e.g. Findell and Eltahir, 2003) that a possible explanation for a negative feedback in a dry soil case might be triggered by a quickly growing PBL (larger sensible heat fluxes) which eventually surpasses the elevation of the LCL and LFC levels which are at a higher altitude in a drier soil condition. On the other hand, a wetter soil condition would lead to less vigourous PBL growth even though LCL and LFC are at a lower altitude. Analysis reveals some localised differences among CTRL, DRY and WET simulations (i.e. smaller difference between PBL and LFC and PBL and LCL), particularly in the Kentucky–Tenneesse border and in the Indiana and Ohio regions. This is consistent with CAPE differences shown before. However, overall, the changes are minimal and are not as clear cut as those shown for CAPE, particularly early in the morning. At this point, the reasons for the results obtained here related to precipitation remain elusive since CAPE does not constitute an explanation but a diagnostic. We are of the opinion that the current explanations in the literature (e.g. Findell and Eltahir, 2003) for soil moisture precipitation feedback have been made with localised convection in mind and with little or no synoptic forcing. We suggest that the mechanisms that are at work during moderate to strong synoptic forcing may modify the pathway through which the feedbacks take place in subtle but important ways.

Inspection of horizontal wind fields for both CTRL - DRY and CTRL - WET differences (Fig. 2b and c) near the surface and vertical velocity aloft (700 hPa) (not shown) revealed that in several instances, regions of wind divergence (convergence) near the surface appeared co-located with decreasing (increasing) precipitation. Near the surface, wind differences in magnitude reached values up to 2 m s^{-1} or more near the locations where precipitation activity was most prominent while outside the region of convective activity the wind speed was reduced to less that 0.5 m s^{-1}.

The difference between the CTRL run and the average of the *12 dry and wet ensemble members* (ENS) showed that the effect of combining the DRY and WET ensembles seemed to cancel the dry and wet biases introduced separately in the precipitation differences over South Central Kentucky (not shown). An interesting non-linear behaviour was noted in regions where the 24-h accumulated precipitation was larger than about 40 mm in the CTRL run (Fig. 2a). In these regions, *both* the DRY and WET ensembles with respect to the CTRL simulation reported reduced precipitation in the range of 20–30 mm (Fig. 2b and c).

Upper-level soil moisture (0–10 cm) for the CTRL simulation on 12 June 0400 UTC shows higher values over Kentucky as expected from the simulated precipitation pattern (Fig. 3a). Due to experimental design, the differences in CTRL – DRY simulations, soil moisture were largely positive in the entire domain from the start of the simulations (Fig. 3b). Similarly CTRL – WET simulations were largely negative (Fig. 3c). Over most of study regions, soil moisture
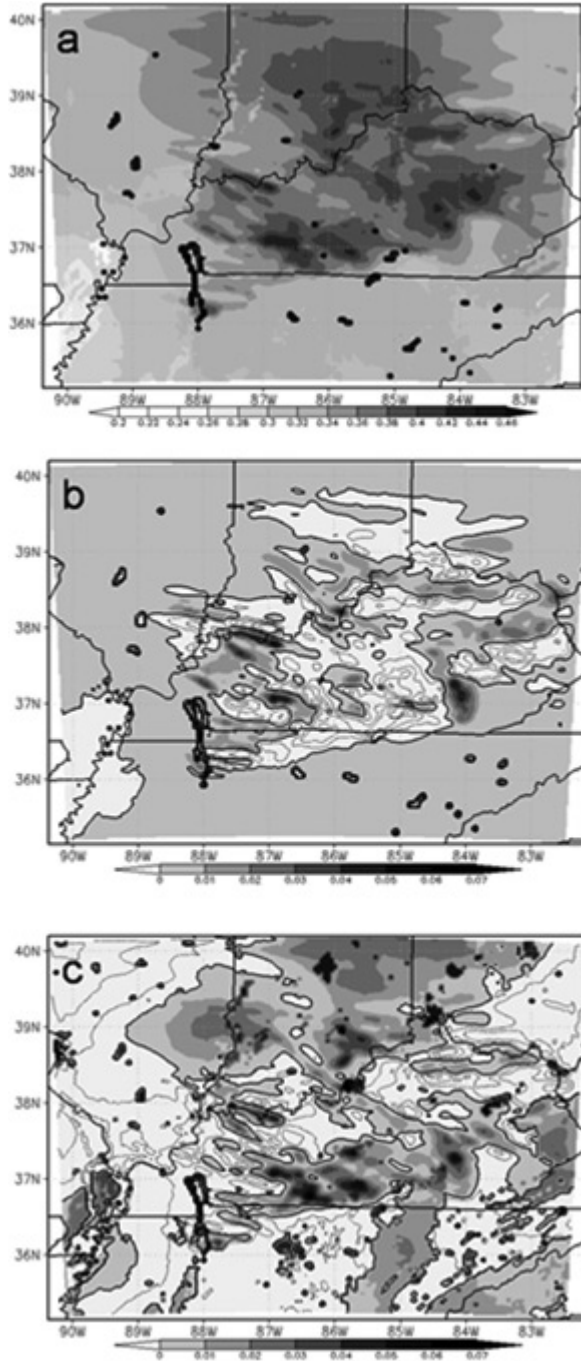
Fig. 3. (a) Volumetric soil moisture ($m^3 m^{-3}$) for the CTRL run for the upper model layer (0–10 cm) on 12 June 0400 UTC; (b) CTRL minus the ensemble average of DRY runs and (c) for the CTRL minus the ensemble average of WET run.

response resembled, to a noticeable extent, the response patterns of precipitation (Fig. 2b and c). These results suggest that local soil moisture changes were driven by precipitation changes for these short-term integrations during this synoptic event.

We suggest that since initial soil moisture level was high, drying changed energy partitioning in a manner that it enhanced precipitation in many areas within South Central and Eastern Kentucky. On the other hand, there were also areas where drying of soils resulted in lowering of precipitation. Comparatively, outside of Kentucky, the model showed a very weak response to soil moisture change which suggested that only the regions where convective activity was present in the CTRL simulation became affected by soil moisture change (Fig. 2b).

The spatial spread between CTRL and the DRY and WET ensembles and the entire 12 member ensemble (ENS) were shown in Figs. 4a–c, 5a–c and 6a–c, for relative humidity (RH), temperature (T), vertical velocity (W), respectively, at the 960 hPa level. As stated in previously each figure includes only three of the four stated metrics namely, normalised RMSD′, normalised bias B and normalised standard deviation.

Figures 4a and 5a show the RMSD' for the pairs (CTRL, DRY), (CTRL, WET) and (CTRL, ENS). RH had the largest RMSD' reaching about 0.6 of the standard deviation of CTRL on 12 June at about 0600 UTC. The RMSD' for T, however, was barely 0.2 at about the same time. Figure 4b and 5b show the bias B for RH and T, respectively. The time evolution of the pair (CTRL, DRY) was almost always negatively correlated with the corresponding bias for (CTRL, WET). The pair (CTRL, ENS) was closer to zero which indicated that inclusion of all ensemble members could cancel the bias. Figures 4c and 5c show normalised standard deviations for RH and T to be close to one which indicated that the amplitude of the fields was very similar to that of CTRL.

A very different behaviour was noted for the W (Fig. 6). It was found that R values decreased significantly to about 0.5 and 0.4 on 12 June at 0400 UTC for all pairs (not shown). Corresponding RMSD' values, on the other hand, increased to reach almost one standard deviation of the CTRL (Fig. 6a) and its bias B was almost zero during the period of integration (Fig. 6b). Finally, Fig. 6c shows the normalised standard deviation of all pairs decreased to 0.5. This represented an approximate 50% decrease of the standard deviation of the DRY, WET and ENS ensembles with respect to the standard deviation of the CTRL. A similar analysis was performed for the horizontal wind components and soil moisture. These variables displayed a similar behaviour (not shown here) as the one presented here for RH and T.

3.2. *17 June 2006*

This event took place over Southern Illinois and Indiana with precipitation amounts exceeding 50 mm (not shown). The 24-h average wind was mostly southerly at 960 hPa.

Relative humidity (960 hPa) June 11-12
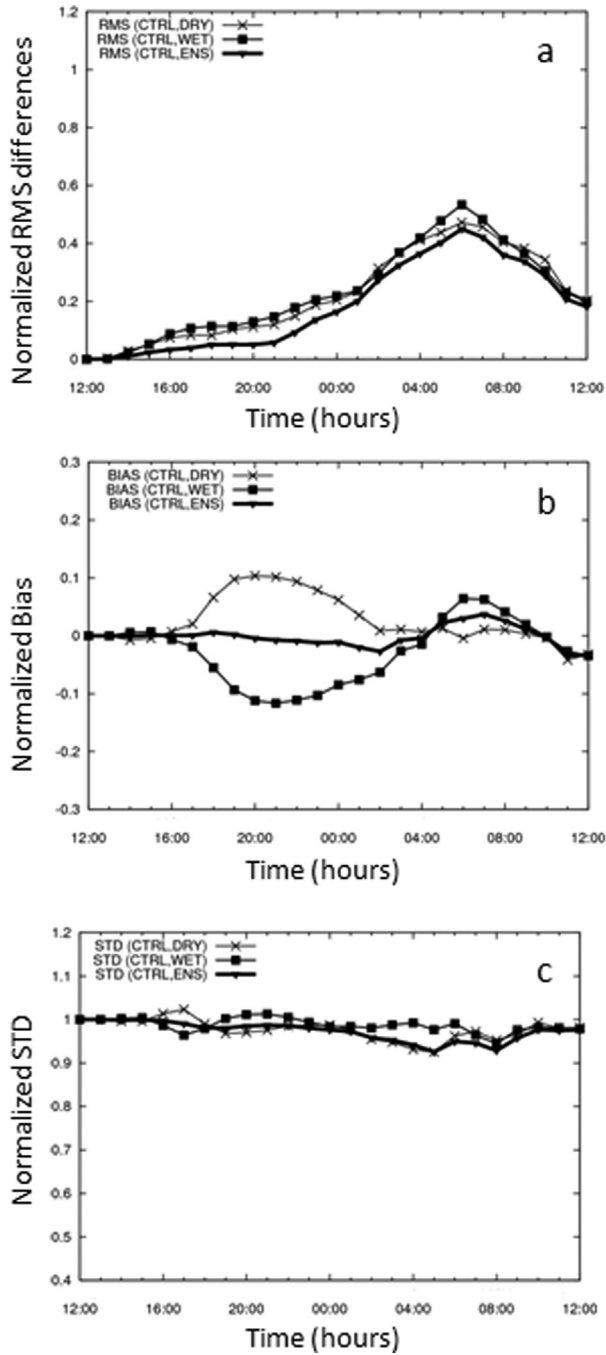

Temperature (960 hPa) June 11-12

Fig. 4.   (a) Time series for RMSD' between CTRL and DRY ensemble (thin line and cross symbol), CTRL and WET ensemble (thin line and square symbol), CTRL and ENS (thick line and triangle symbol) for relative humidity at 960 hPa; (b) normalised bias *B* and (c) normalised standard deviation σ for 11–12 June 2006.
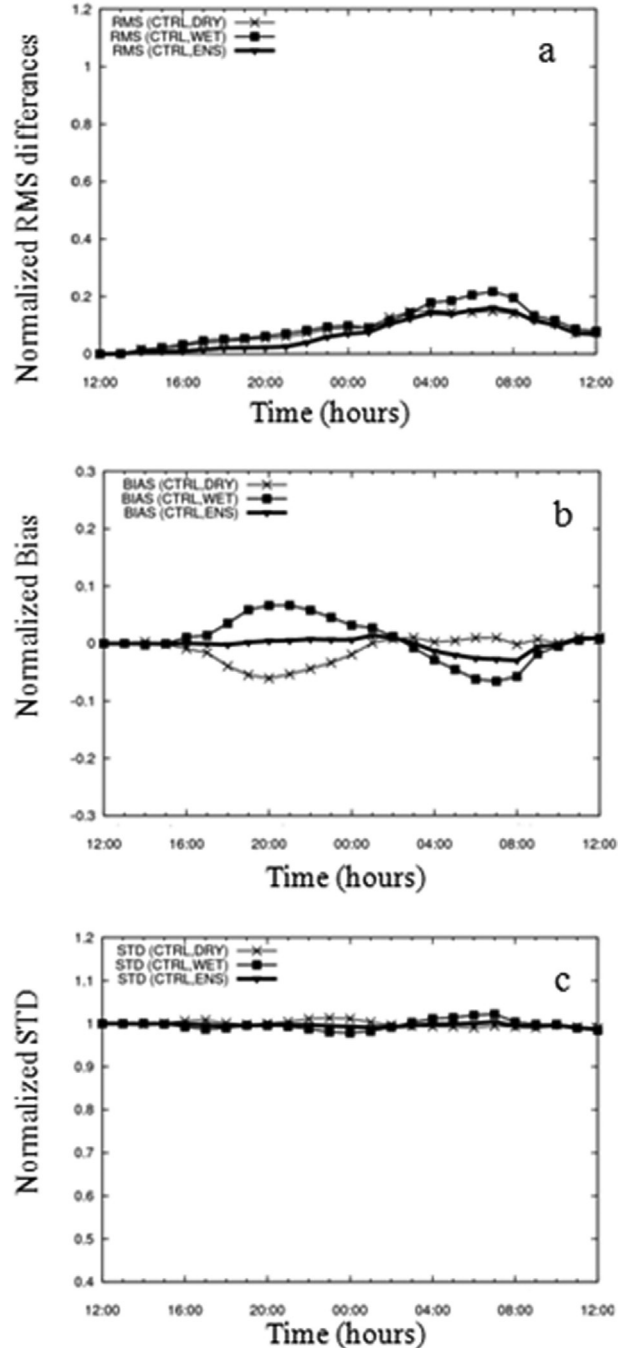
Fig. 5.   As in Fig. 4 but for temperature at 960 hPa.

As in the previous case, the response in precipitation and wind field was confined mostly to the regions where precipitation was high, particularly along the rain bands in

the northwest corner of the inner domain. Like 11 June case, in some areas within the domain precipitation was increased and decreased in the CTRL – DRY and CTRL – WET differences (not shown). Again, these were existing areas (i.e. CTRL) of relatively larger amount of precipitation. The CTRL – ENS continued to show this particular
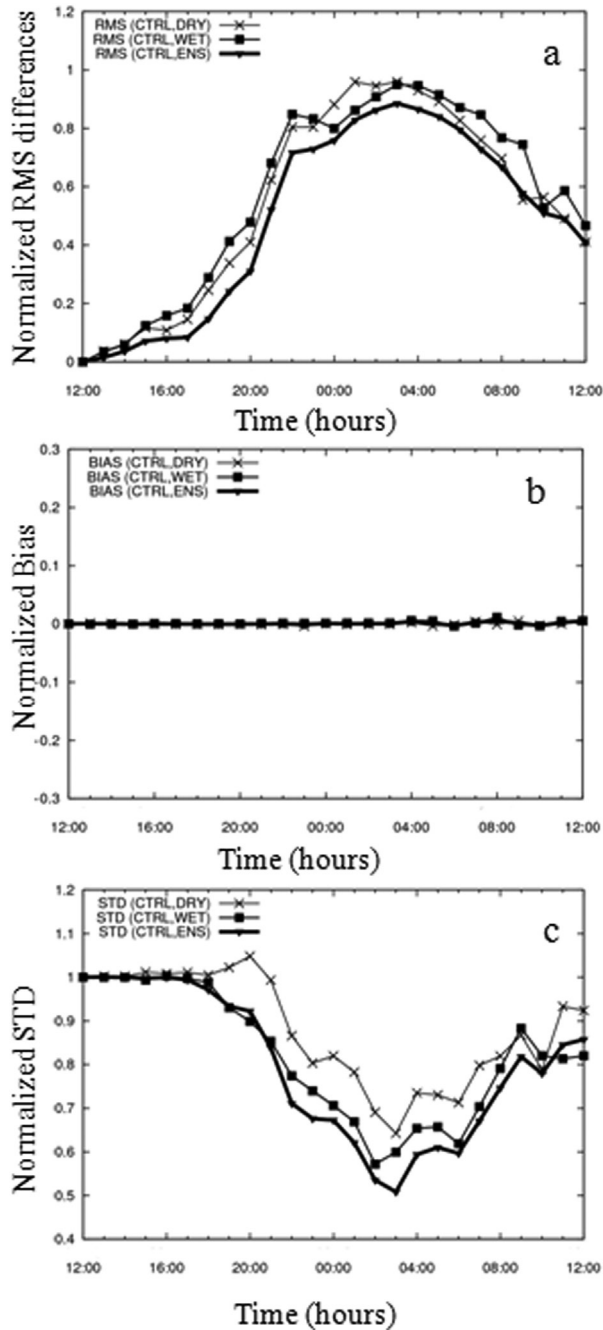
Vertical Velocity (960 hPa) June 11-12

Fig. 6. As in Fig. 4 but for vertical velocity at 960 hPa.

in the CTRL - WET difference and in fact it appeared to be the case for the entire domain where changes in precipitation rates were very small compared to the main convective regions. These results suggested that the effects of drying and wetting the soil led to a small negative feedback effect in precipitation for both DRY and WET simulations and crucially depended on the previous convective state and the intensity of the precipitation rates. Finally, in contrast to the 11 June case the 24-h average wind differences show magnitudes not larger than 2 m s^{-1} even at locations where precipitation has larger values.

Upper-level soil moisture (0–10 cm) for the CTRL simulation of 18 June 0400 UTC was analysed and higher soil moisture content were located over Southern Illinois and Indiana and Western Kentucky, as expected from simulated spatial distribution of precipitation. The areas of large positive change in soil moisture were found to be co-located with correspondingly large precipitation changes. As discussed previously, comparison of precipitation patterns suggested that precipitation changes drive soil moisture changes in the same direction. Visual inspection found that the CTRL – DRY and CTRL – WET differences were spatially negatively correlated with each other as noted previously in the 11 June case.

Spatial spread between the CTRL, DRY, WET and ENS ensembles for RH, T and W at the 960 hPa level, respectively, were assessed. The largest RMSD' for RH was about 0.6 and it was observed on 18 June at about 0000 UTC. The RMSD' for T, however, was about 0.2 at about the same time. The normalised bias B for RH and T showed similar behaviour as found in the 11 June case but at least three to four times larger (not shown). The normalised standard deviations for RH and T for the three pairs were found to differ slightly among the DRY and WET experiments particularly on June 2000 UTC when values of B among the experiments also differed. Inspection of the corresponding statistics for the vertical velocity field revealed an almost identical behaviour as that encountered for the 11 June case.

3.3. 11 June 2006

During this event significant precipitation occurred in Illinois and Indiana with amounts exceeding 50 mm (Fig. 7a). It was also found that 24-h average horizontal wind was mostly southerly at 960 hPa (Fig. 7a). Figure 7b and c shows precipitation response from the DRY, and WET experiments, respectively. In comparison to the 11 June case the response in precipitation and wind was rather modest for this period near the convective regions. Once again the most active convective regions show a decrease in precipitation with respect to the CTRL simulation, as found in the two previous cases. Moreover, reversal of precipitation response between DRY and

precipitation change pattern (not shown). Of note, is a region in Central Kentucky (86–88°W and 37–38°N) where southwest to northeast oriented rain bands had a less than 5 mm increase in precipitation (CTRL – DRY). Adjacent to this region in the west, there is a region where precipitation rates were decreased with respect to the CTRL by small amount as well (less than 5 mm). This pattern was reversed
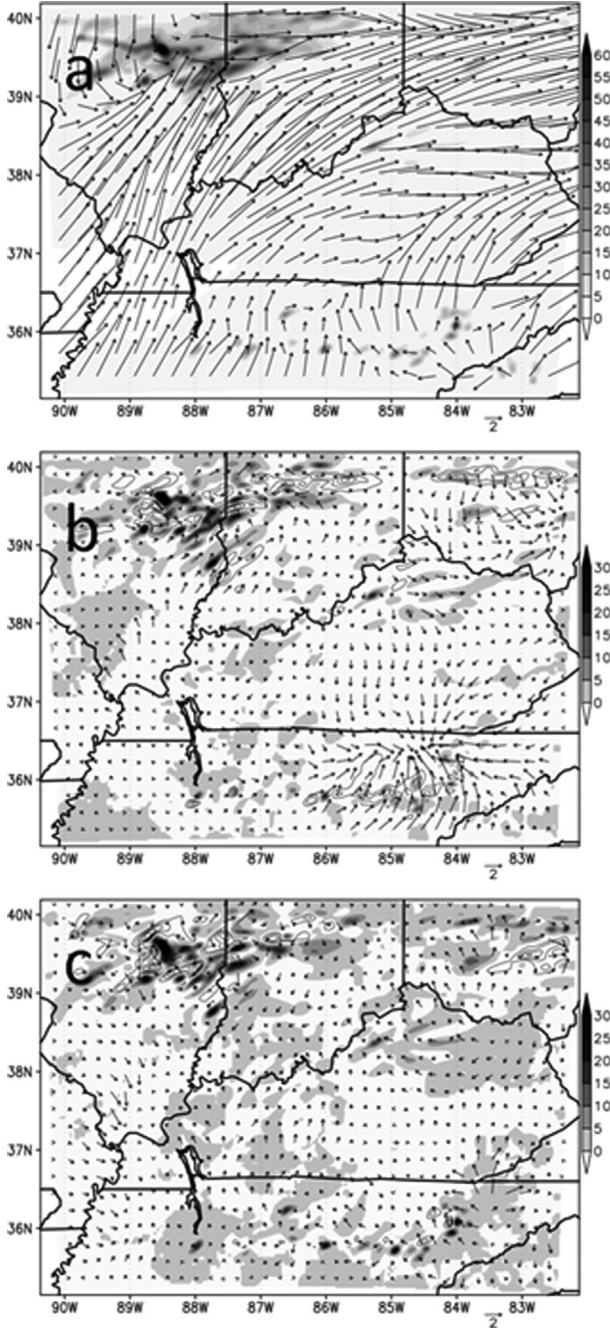
Fig. 7.   As in Fig. 2 (24-h accumulated precipitation and wind) but for the period of 22 June 1200 UTC through 23 June 1200 UTC.

WET simulations was noted. For example, over southwest Illinois precipitation shows a decrease under DRY ensembles while increase or no change for WET ensembles. Furthermore, visual inspection suggests that precipitation decrease was more prevalent for WET simulations.

As for the wind, in the CTRL – DRY (Fig. 7b), a large response was found in the Northeastern Tennessee. Here, a

region of converging winds can be indentified with wind difference reaching up to speed of 4 m s^{-1}. This wind feature could not be found in the CTRL – WET difference.

Analysis showed higher soil moisture (10 cm depth from the surface) content for the CTRL simulation on 23 June 0400 UTC over Illinois, Indiana and Kentucky (Fig. 8a). It is found that the areas of large positive change in soil moisture were to be co-located with corresponding large precipitation changes as noted in the previous cases (Fig. 8b and c). As in the two previous precipitation cases, for this strong convective activity, visual inspection suggests that the CTRL – DRY and CTRL – WET soil moisture differences were spatially negatively correlated.

Figures 9a–c, 10a–c and 11a–c show the spatial spread between the CTRL, DRY and WET ensembles for RH, T and W at the 960 hPa level, respectively. Figures 9a and 10a show the RMSD' for the pairs (CTRL, DRY), (CTRL, WET) and (CTRL, ENS). Again, RH had the largest RMSD reaching about 0.6 on 23 June at 0800 UTC. The RMSD' for T was about 0.4 for this time and slightly larger than its counterparts for 11 and 17 June.

As in the 11 and 17 June cases, the B for the RH and T and for the CTRL and DRY pair evolved in opposite directions compared to the corresponding B for CTRL and WET (Figs. 9b and 10b). The pair CTRL and ENS was closer to zero. It is found that the normalised standard deviations for RH and T were close to 1 which indicated that the amplitude of the fields was very similar to that of CTRL (Fig. 9c and 10c). Inspection of the corresponding statistics for the vertical velocity field (Fig. 11a–c) revealed similar behaviour as that encountered for the 11 and 17 June cases.

3.4. Vertical dependence of pattern statistics

In order to show how the RMSD' statistics of the pair (CTRL, ENS) varied with height, Fig. 12 shows these quantities as a function of the model's vertical coordinate (sigma) for 12 June 0400 UTC (Fig. 12a), 18 June 0400 UTC (Fig. 12b) and 23 June 0400 UTC (Fig. 12c). Inspection of these figures revealed that the vertical velocity was most sensitive to soil moisture perturbations for the entire atmospheric column and in agreement with the temporal evolution of RMSD'. Values of RMSD' for vertical velocity increased from 0.0 to 1.0 for 22 June (Fig. 12c). RH, T and the horizontal wind field, did not show, on the other hand, such sensitivity.

Hence, soil moisture perturbation could produce sufficient spread for vertical velocity but not for RH, T and horizontal wind field. Sutton et al. (2006) noted that soil moisture is capable of producing significant spread in ensemble simulations while Aligo et al. (2007) indicated that there is only marginal impact of soil moisture on ensemble spread. Our results suggest that spread of vertical
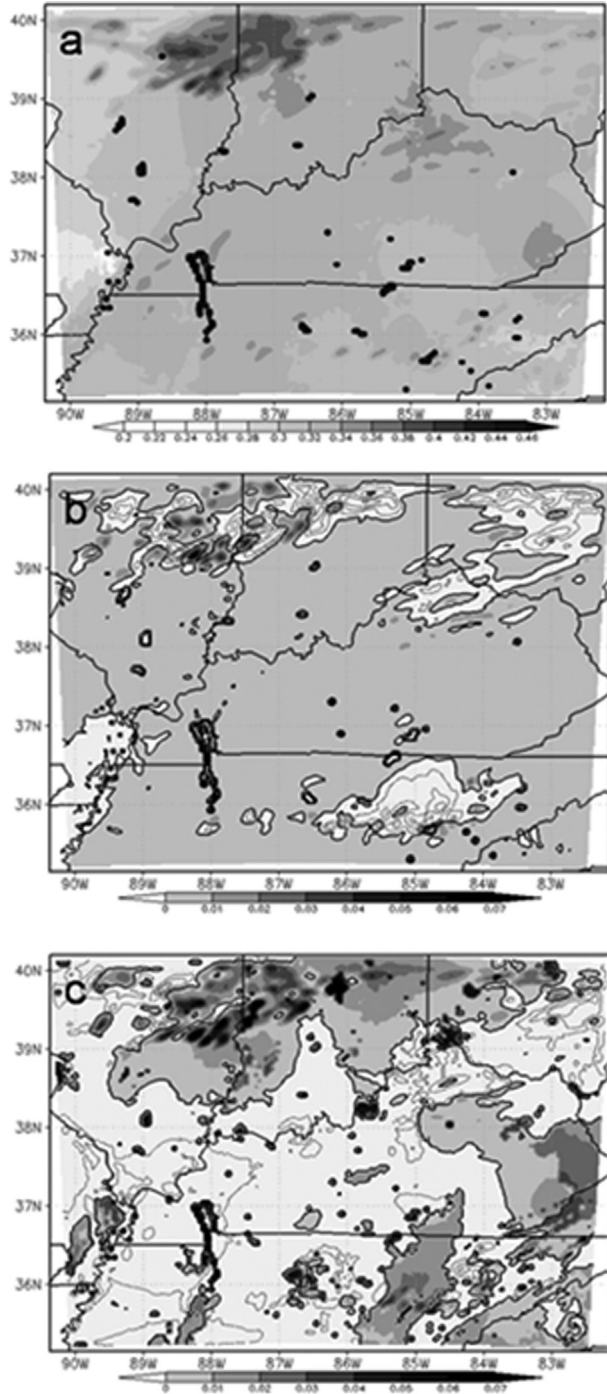
Fig. 8. As in Fig. 3 but for 23 June 0400 UTC.

velocity is notable and is linked to precipitation. In addition, these changes were clearly a response to soil moisture perturbations. The findings from three synoptic conditions suggest that the results are general and needs further investigation.
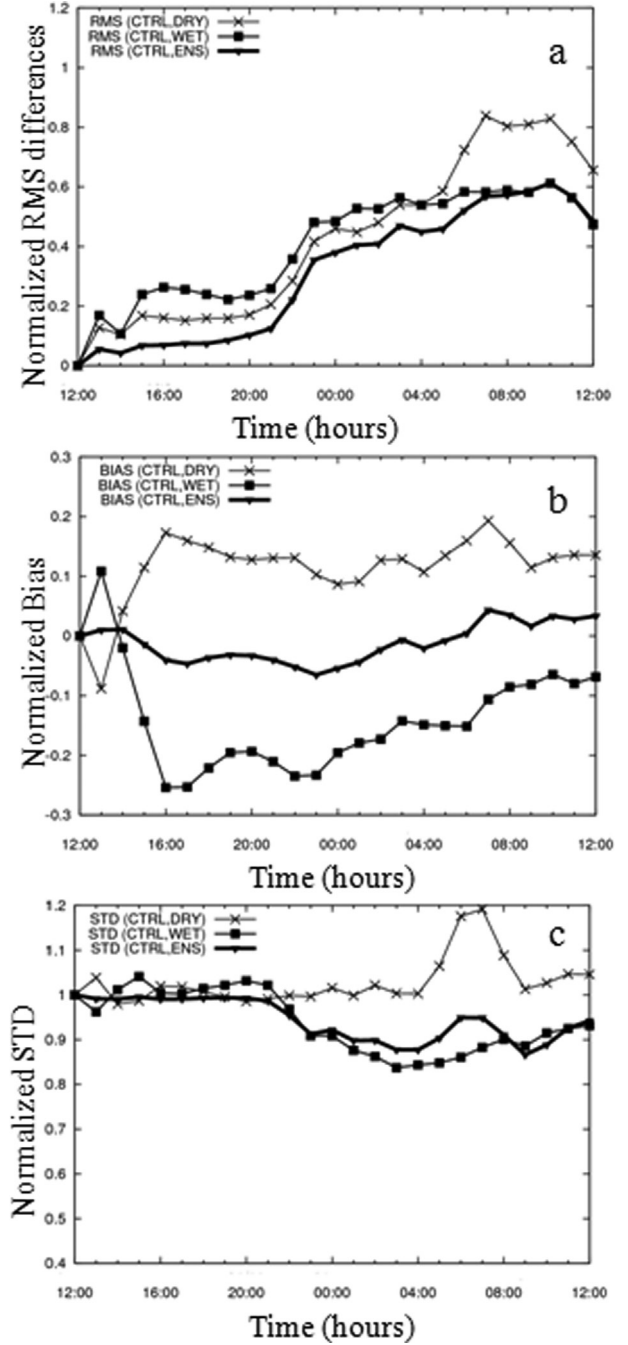

Fig. 9. As in Fig. 4 but for relative humidity at 960 hPa for the period of 22 June 1200 UTC through 23 June 1200 UTC.

4. Final remarks

The principal aim of this research was to diagnose the spread of an ensemble forecast simulations using a measure of spatial dispersion between forecast ensemble members
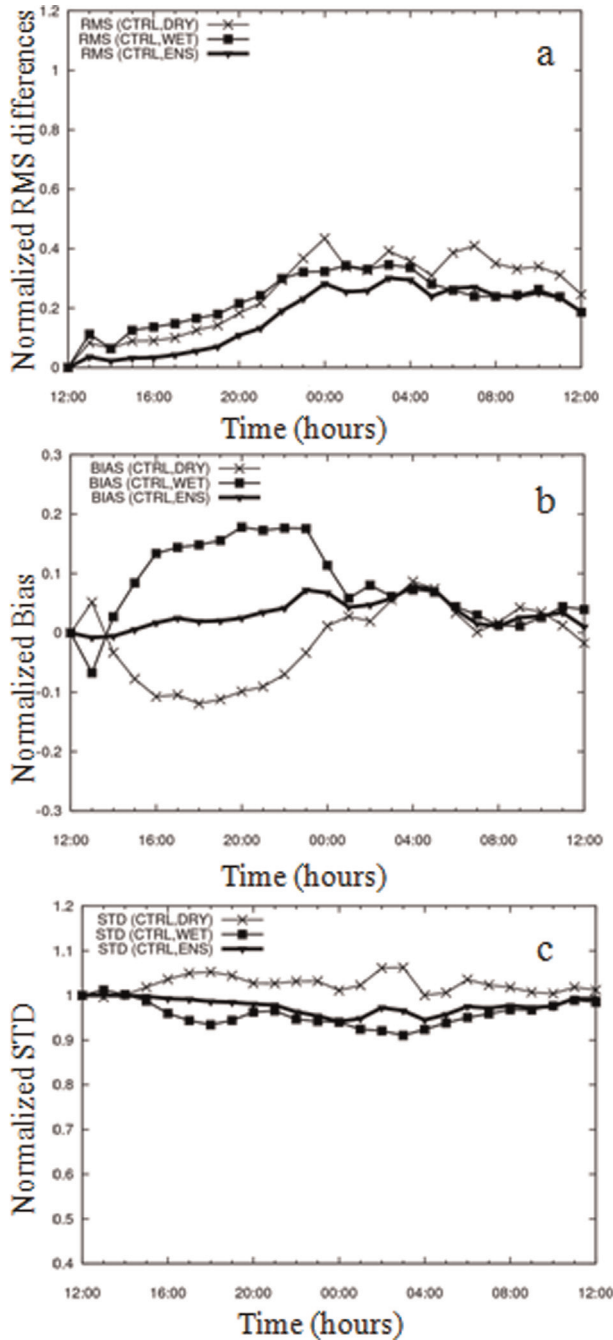
Fig. 10.   As in Fig. 4 but for temperature and for the period of 22 June 1200 UTC through 23 June 1200 UTC.

and control simulations. An ensemble of 12, 24-h simulations was generated from soil moisture perturbations over the entire model domain for three different synoptic conditions of different strengths. This study has used several measures of statistical spatial dispersion, namely, the normalised RMSD', the normalised standard deviation (σ), the normalised bias (B) and the spatial correlation
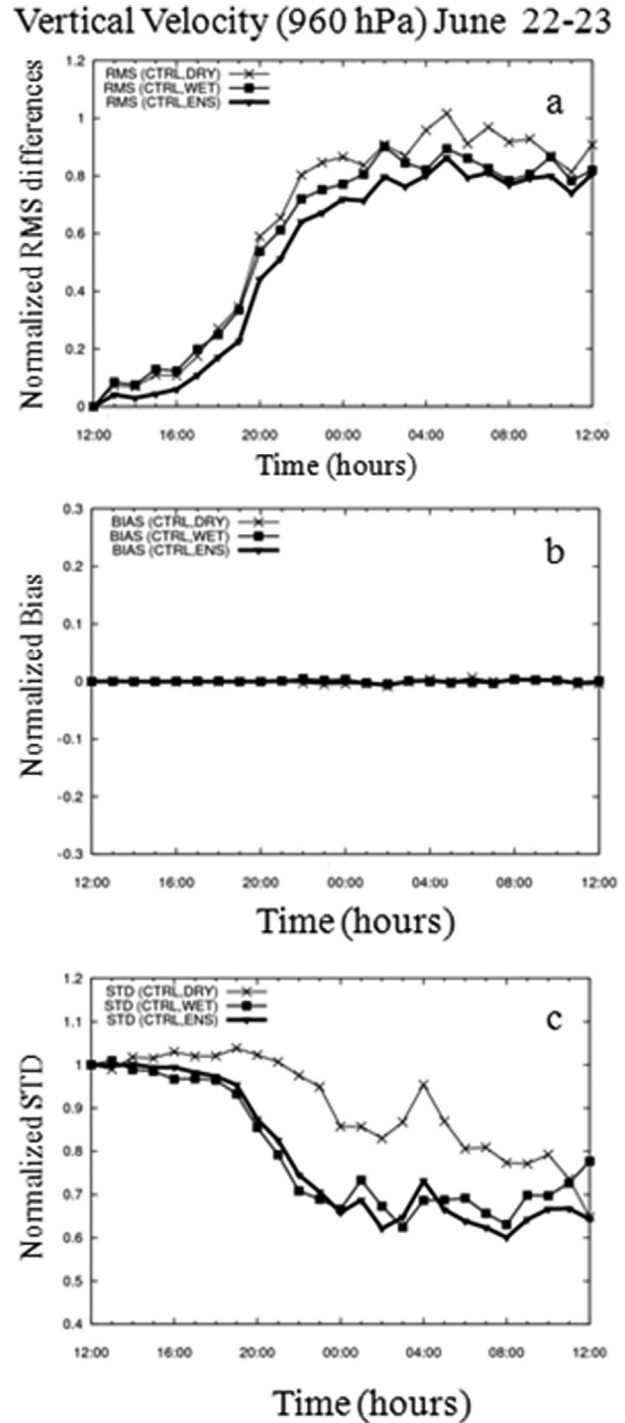

Fig. 11.   As in Fig. 4n but for vertical velocity and the period of 22 June 1200 UTC through 23 June 1200 UTC.

coefficient (R) to determine time evolution of ensemble member spread for temperature, relative humidity and wind field. It was found that drying and wetting of soil moisture has an important impact on precipitation. However, it is depended on initial soil moisture content of the
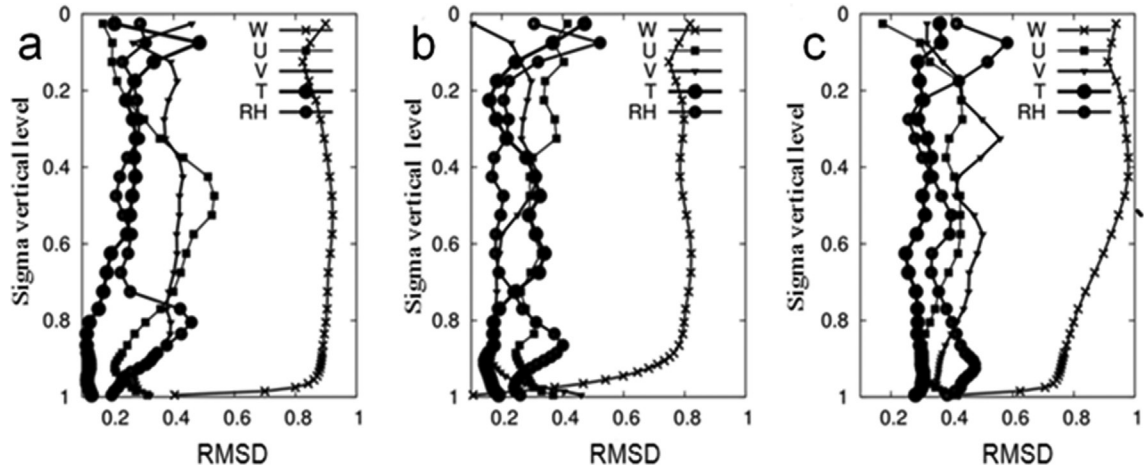
Fig. 12. RMSD′ as function of the model vertical coordinate (sigma) for (a) 11 June 0400 UTC; (b) 17 June 0400 UTC and (c) 22 June 0400 UTC. Variables correspond to vertical velocity (W), zonal wind component (U), meridional wind component (V), temperature (T) and relative humidity (RH).

land surface. This study found that in some areas within the inner domain DRY ensembles resulted in higher precipitation where WET ensembles suppressed precipitation. It occurred for all synoptic conditions indicating that a negative soil moisture precipitation feedback was present over most of the computational domain excluding localised precipitation areas in the CTRL simulation where the DRY experiments showed a positive feedback. We suggest that since CTRL soil moisture was already relatively high and subsequent drying and wetting of soils changed the land surface condition in such a way that it affected vertical velocity and thus increased or decreased precipitation. This is certainly consistent with the spread of vertical velocity we have found with soil moisture perturbations. As a result, we suggest that the soil moisture perturbations alone might be an important contributor to the spread of ensemble forecasting system. Additional analysis of for CAPE, PBL, LCL and LFC was completed to understand mechanisms that led to changes in precipitation. For example, it was found increase in CAPE under DRY simulations which is consistent with our negative soil moisture-precipitation feedback. It is also found that differences between PBL and LCL and PBL and LFC became smaller along with convective development as day progressed. However, these changes were not as large as shown by CAPE. Moreover, again, PBL and LCL and PBL and LFC differences were not as large as shown by Findell and Eltahir (2003). We suspect, in our case, significant synoptic (as opposed to localised convective events) activities removed some these signatures from the simulations. Moreover, we also note that additional research needs to be conducted to further understand the role of wet soils on precipitation development.

These statistics also revealed that temperature, relative humidity and the horizontal wind field are modestly sensitive to soil moisture perturbations. In other words, soil moisture perturbations can produce sufficient spread in ensembles of vertical velocity (thus, precipitation) but not for RH, T and horizontal winds. Hence, it can be said that the present study has provided further insight into the impacts soil moisture perturbations on ensemble spread. We agree with Aligo et al. (2007) and Sutton et al. (2006) that additional experiments need to be undertaken where soil moisture and atmospheric initial conditions perturbations and model physics will be considered simultaneously. Moreover, further soil moisture-atmosphere observational and modelling work may reveal mechanisms that control localised precipitation under variety of conditions, which could be useful to understand ensemble spreads. It is expected that this type of comprehensive study will improve our knowledge in ensemble spread, causes of model behaviour and thus short-term forecasts.

5. Acknowledgements

References

Aligo, E., Gallus, W. and Segal, M. 2007. Summer rainfall forecast spread in an ensemble initialized with different soil moisture analyses. *Weather Forecast.* **22**, 299–314.

Balsamo, G., Mahfouf, J., Belair, S. and Deblonde, G. 2007. A land data assimilation system for soil moisture and temperature: an information content study. *J. Hydrometeorol.* **8**, 1225–1242.

Betts, A. K., Ball, J. H., Beljaars, A. C. M., Miller, M. J. and Viterbo, P. A. 1996. The land surface–atmosphere interaction: a review based on observational and global perspectives. *J. Geophys. Res.* **101**, 7209–7225.

Bosilovich, M. G., Chen, J., Robertson, F. R. and Adler, R.F. 2008. Evaluation of global precipitation reanalyses. *J. Appl. Meteor. Clim.* **47**, 2279–2299.

Capprini, F. and Castelli, F. 2004. Estimation of surface turbulent fluxes through assimilation of radiometric surface temperature sequences. *J. Hydrometeorol.* **5**, 145–159.

Chang, H.-I., Niyogi, D., Kumar, A., Kishtawal, C. M., Dudhia, J. and co-authors. 2009. Possible relation between land surface feedback and the post-landfall structure of monsoon depressions. *Geophys. Res. Lett.* **36**, L15826. DOI: 10.1029/2009GL037781.

Chen, F. and Avissar, R. 1994. Impact of land-surface moisture variability on local shallow convective cumulus and precipitation in large-scale models. *J. Appl. Meteor.* **33**, 1382–1401.

Chen, F. and Dudhia, J. 2001. Coupling an advanced land surface-hydrology model with the Penn State-NCAR MM5 modeling system. Part I: model implementation and sensitivity. *Mon. Weather Rev.* **129**, 934–958.

Crook, A. N. 1996. Sensitivity of moist convection forced by boundary layer to low-level thermodynamic fields. *Mon. Weather Rev.* **124**, 1767–1785.

Diak, G., Heikkinen, S. and Bates, J. 1986. The influence of variations in surface treatment on 24-hour forecasts with a limited area model, including a comparison of modeled and satellite measured surface temperatures. *Mon. Weather Rev.* **114**, 215–232.

Dong, J., Ni-Meister, W. and Houser, P. R. 2007. Impacts of vegetation and cold season processes on soil moisture and climate relationships over Eurasia. *J. Geophys. Res.* **112**, 1–11.

Duffy, P. B., Arrit, R. W., Coquard, J., Gutowski, W., Han, J. and co-authors. \2006. Simulations of present and future climates in the Western United States with four nested regional climate models. *J. Clim.* **19**, 873–895.

Ek, M. and Mahrt, L. 1994. Daytime evolution of relative humidity at the boundary layer top. *Mon. Weather Rev.* **122**, 2709–2721.

Fast, J. and McCorcle, M. D. 1991. The effect of heterogeneous soil moisture on a summer baroclinic circulation in the Central United States. *Mon. Weather Rev.* **119**, 2140–2167.

Findell, K. and Eltahir, E. A. B. 2003. Atmospheric control in soil moisture–boundary layer interactions: three-dimensional winds effects. *J. Geophys. Res.* **108**, D88385. DOI: 10.1029/2001JD001515.

Hamill, T. M. and Colucci, S. J. 1997. Verification of Eta–RSM short-range ensemble forecasts. *Mon. Weather Rev.* **125**, 1312–1327.

Hong, S.-Y. and Pan, H.-L. 1996. Nonlocal boundary layer vertical diffusion in a medium-range forecast model. *Mon. Weather Rev.* **124**, 2322–2339.

Jolliff, J. K., Kindle, J. C., Shulman, I., Penta, B., Friedrichs, M. A. M. and co-authors. 2009. Summary diagrams for coupled hydrodynamic-ecosystem model skill assessment. *J. Mar. Syst.* **76**, 64–82.

Kain, J. 2004. The Kain–Fritsch convective parameterization: an update. *J. Appl. Meteor.* **43**, 170–181.

Kalnay, E. 2003. *Atmospheric Modeling, Data Assimilation and Predictability*. Cambridge University Press, Cambridge. 341 pp.

Koster, R. D. and Suarez, M. J. 1996. *Energy and water balance calculations in the mosaic LSM*. NASA Tech. Memo. 104606, **9**(59), 140.

Koster, R., Dirmeyer, P. A., Guo, Z., Bonan, G., Chan E. and co-authors. 2004. Regions of strong coupling between soil moisture and precipitation. *Science* **305**, 1138–1140.

Legates, D. R., Mahmood, R., Levia, D. F., DeLiberty, T. D., Quiring, S. and co-authors. 2011. Soil moisture: a central and unifying theme in physical geography. *Prog. Phys. Geogr.* **35**, 65–86.

Li, S., Goddard, L. and DeWitt, D. G. 2008. Predictive skill of AGCM seasonal climate forecasts subject to different SST prediction methodologies. *J. Clim.* **10**, 2169–2186.

Mahmood, R. and Hubbard, K. G. 2004. An analysis of simulated long-term soil moisture data for three land uses under contrasting hydroclimatic conditions in the Northern Great Plains. *J. Hydrometeorol.* **5**, 160–179.

Ookouchi, Y., Segal, M., Kessler, R. C. and Pielke, R. A. 1984. Evaluation of soil moisture effects on the generation and modification of mesoscale circulations. *Mon. Weather Rev.* **112**, 2281–2292.

Palmer, T. N., Alessandri, A., Anderson, U., Cantelaube, P., Davey, M. and co-authors. 2004. Development of a European multimodel ensemble system for seasonal-to-interannual prediction (DEMETER). *Bull. Am. Meteorol. Soc.* **85**, 853–872.

Pielke, R. A. Sr., 2001. Influence of the spatial distribution of vegetation and soils on the prediction of cumulus convective rainfall. *Rev. Geophys.* **39**, 151–177.

Quintanar, I. A., Mahmood, R., Loughrin, J. and Lovanh, N. C. 2008. A coupled MM5-NOAH land surface model-based assessment of sensitivity of planetary boundary layer variables to anomalous soil moisture conditions. *Phys. Geogr.* **29**, 54–78.

Sasamori, T. 1970. A numerical study of atmospheric and soil boundary layers. *J. Atmos. Sci.* **27**, 1122–1137.

Santanello, J. A., Peters-Lidard, C. D., Kumar, S. V., Alonge, C. and Tao, W.-K. 2009. A modeling and observational framework for diagnosing local land–atmosphere coupling on diurnal time scales. *J. Hydrometeorol.* **10**, 577–599.

Santanello, J. A., Peters-Lidard, C. D. and Kumar, S. V. 2011. Diagnosing the sensitivity of local land-atmosphere coupling via the soil moisture–boundary layer interaction. *J. Hydrometeorol.* **12**, 766–786, DOI: 10.1175/JHM-D-10-05014.1.

Schär, C., Luthi, D. and Beyerle, U. 1999. The soil-precipitation feedback: a process study with a Regional Climate Model. *J. Clim.* **12**, 722–741.

Senevirante, S. I., Corti, T., Davin, E. L., Hirschi, M., Jaeger, E. B. and co-authors. 2010. Investigating soil-moisture climate interactions in a changing climate: a review. *Earth Sci. Rev.* **99**, 125–161.

Stensrud, D. J., Bao, J.-W. and Warner, T. T. 2000. Using initial condition and model physics perturbations in short-range ensemble simulations of mesoscale convective systems. *Mon. Weather Rev.* **128**, 2077–2107.

Sutton, C., Hamill, T. and Warner, T. 2006. Will perturbing soil moisture improve warm-season ensemble forecasts? A proof of concept. *Mon. Weather Rev.* **134**, 3174–3189.

Taylor, C. M., Saïd, F. and Lebel, T. 1997. Interactions between the land surface and mesoscale rainfall variability during HAPEX-Sahel. *Mon. Weather Rev.* **125**, 2211–2227.

Taylor, K. 2001. Summarizing multiple aspects of model performance in a single diagram. *J. Geophys. Res.* **106**, 7183–7192.

Taylor, C. M. and Ellis, R. J. 2006. Satellite detection of soil moisture impacts on convection at the mesoscale. *Geophys. Res. Lett.* **34**, L03404. DOI: 10.1029/2005GL025252.

Taylor, C. M., Parker, D. J. and Harris, P. P. 2007. An observational case study of mesoscale atmospheric circulations induced by soil moisture. *Geophys. Res. Lett.* **34**, L15801. DOI: 10.1029/2007GL030572.

Teuling, A., Uijlenhoet, R., Hupet, F. and Troch, P. 2006. Impact of plant water uptake strategy on soil moisture and evapotranspiration dynamics during drydown. *Geophys. Res. Lett.* **33**. L03401–4, DOI: 10.1029/2005GL025019.

Tjernström, M., Zăgar, M., Svensson, G., Cassano, J. J., Pfeifer, S. and co-authors. 2005. Modelling the arctic boundary layer: an evaluation of six ARCMIP regional-scale models using data from the SHEBA project. *Boundary-Layer Meteorol.* **117**, 337–381.

Toth, Z., Kalnay, E., Tracton, S., Wobus, R. and Irwin, J. 1997. A synoptic evaluation of the NCEP ensemble. *Weather Forecast.* **12**, 140–153.

Tracton, M. S. and Kalnay, E. 1993. Ensemble forecasting at NMC: the generation of perturbations. *Bull. Am. Meteorol. Soc.* **74**, 2317–2330.

Yang, F., Kumar, K. and Lau, K.-M. 2004. Potential predictability of U.S. summer climate with ''perfect'' soil moisture. *J. Hydrometeorol.* **5**, 883–895.